JOURNAL OF PROPULSION AND POWER
Vol. 20, No. 1, January–February 2004

Intermittent Burning of Ammonium Perchlorate–Hydrocarbon Binder Monomodal Matrixes, Sandwiches, and Propellants

Satyanarayanan R. Chakravarthy,* Jerry M. Seitzman,† Edward W. Price,‡ and Robert K. Sigman§
Georgia Institute of Technology, Atlanta, Georgia 30332-0150

The onset of the midpressure extinction of certain formulations (termed matrixes) of ammonium perchlorate (AP) of monomodal particle size distribution and hydroxyl–terminated polybutadiene binder, in the pressure range around 2–5 MPa, is examined. These matrixes, besides being tested in isolation, have been included in between AP laminas to form sandwiches and mixed with coarse AP particles to form high solids-loading (87.5%) non-aluminized propellants. The burning rates of the sandwiches show abnormal trends with pressure such as low or negative exponents in ranges corresponding to the onset of the midpressure extinction of their respective matrixes. The propellants exhibit this behavior to a lesser degree. Quenched surfaces (self-extinguished or intentionally interrupted during burning) of all the three types of samples were analyzed using a scanning electron microscope, and the burning history of the samples was captured with a high-speed digital camera. The results indicate the prevalence of intermittent burning of the matrixes as the pressure is varied across the boundary between continuous burning and self-extinction (burn/no-burn boundary) of the matrixes. The burning surfaces are marked by extreme three dimensionality coupled with a redistribution of the fine AP particles and the binder. The observations are explained based on the combined effects of the need for the AP particles and the binder to accumulate relative to each other on the burning surface depending on the difference in their pyrolysis rates and the existence of the binder in a molten state on the burning surface.

Introduction

COMPOSITE solid propellants of the ammonium perchlorate (AP)–hydrocarbon binder class are usually processed with a multimodal AP particle size distribution to achieve high solids loading. A simple approach is to adopt a bimodal distribution, containing coarse and fine AP particles. Of particular interest to this study are those with a wide distribution, wherein a large difference exists between the average diameters of the coarse and fine particles (∼5–200 times). In such a situation, large regions exist between 3–4 adjacent coarse particles in the propellant microstructure, which are filled by a matrix of the fine AP–binder mixture. It has been realized in the past that the burning behavior of the matrix could significantly influence the overall burning behavior of the propellant containing it.[1]

Mixtures of the binder with AP of monomodal particle size distribution have been considered in early research studies to determine the effect of the AP size on their burning rate characteristics.[2,3] Because of packing limitations, these formulations are naturally too fuel rich to be acceptable for rocket propulsion applications. However, the work by Bastress[2] showed some interesting burning behavior of these formulations, such as plateau burning (low- or zero-pressure exponent of burning rate), mesa burning (decreasing burning rate with increase in pressure), and mid-pressure extinction, when very fine AP particles were used, almost regardless of the type of binder. These findings were reconfirmed in a more elaborate study,[3] which included formulations with modest-to-reasonable levels of AP by means of a bimodal particle size distribution. Such burning rate trends deviated from the predictions based on the granular diffusion flame theory proposed earlier.[4] The deviation was explained by recognizing that the binder melted substantially before decomposition and existed in a molten state in the condensed-phase thermal wave. In both these studies,[2,3] irregular burning was noticed in association with such anomalous burning rate trends.

In the context of high solids-loading propellants, Foster and Miller[1] have reported a series of tests in which matrixes of monomodal fine AP particles were compared with propellants containing those matrixes and coarse AP particles to make up for a solids-loading of 86%. One of the matrixes, with 6-μm AP and hydroxyl-terminated polybutadiene (HTPB) in the ratio 77:23, exhibited midpressure extinction, and the corresponding bimodal propellant registered a plateau in that pressure range. Miller[5,6] examined the effect of reducing the AP content to accommodate aluminum in constant solids-loading formulations and relative proportions of the coarse and fine AP fractions. In general, plateau or low-pressure exponent burning rates were observed when the coarse and fine AP sizes were widely spaced and when the coarse AP content was increased. Note that an increase in the coarse AP content at constant solids loading implies a decrease in the fine AP relative to the binder. In all of these works,[1,5,6] the results were explained mainly in terms of an ignition delay for the coarse particles, within the framework of the Beckstead–Derr–Price (BDP) model.[7] No consideration of binder melt flow was made, particularly with regard to the matrixes. However, it was reported that the combustion of propellants proceeded in a somewhat intermittent manner in the plateau burning regime, based on visual observation of the burning event in a macroscopic manner.

On the other hand, Cohen and Hightower[8] have attempted to include the prevalence of molten binder on the burning surface into the framework of the BDP model.[7] They have presented a vast amount of experimental data from a variety of propellant development programs with reasonably complete specifications to highlight those that exhibit anomalous burning rate trends. They identified conspicuous differences in curing agent type, plasticizer contents, etc., and examined the binder melt layer thickness relative to the AP particle size and particle protrusion depth and the melt viscosity effects. The BDP model was used as a tool to diagnose the role of the binder melt layer on the fine AP particles, by neglecting the presence of fine AP in the composition to signify its complete submergence in the binder melt layer in the anomalous burning regime.

Received 29 April 2002; revision received 11 July 2003; accepted for publication 11 July 2003.

*Visiting Scholar, School of Aerospace Engineering; permanently Assistant Professor, Department of Aerospace Engineering, Indian Institute of Technology, Madras, Chennai 600 036, India. Member AIAA.

†Associate Professor, School of Aerospace Engineering. Senior Member AIAA.

‡Regent's Professor Emeritus, School of Aerospace Engineering. Fellow AIAA.

§Senior Research Engineer (retired).

The present work attempts to address two aspects: 1) the nature of the burning surface during intermittent burning of the matrix at the onset of its midpressure extinction and 2) the interaction of the matrix combustion with the oxidizer–fuel (O/F) flame associated with the coarse AP particles in the propellants across the burn/no-burn boundary of the matrix. The latter is examined both by including the matrixes in between two laminas (pressed pellets) of AP to form sandwiches and by mixing the matrixes with coarse AP particles to form bimodal propellants. It is seen from the present work that the sandwiches and propellants exhibit anomalous burning rate trends corresponding to the onset of the midpressure extinction of the matrix contained in them, as reported earlier.[1]

Note that the intermittent burning behavior of the matrix may not always result in anomalous burning rate trends of the propellant containing it, and conversely, plateau burning rates of propellants need not necessarily involve intermittent burning. The former case is discussed in some detail later. As for the latter case, several mechanisms other than those considered here could be involved; steady-state combustion models such as the BDP model[7] can predict plateau-type burning rate characteristics for specific formulations. Also, Chakravarthy et al.[9] have recently reported sandwich and propellant formulations exhibiting plateau burning at elevated pressures and have explained the behavior based on steady-state considerations of the gas-phase flame structure.

Experimental Details

Samples

Three types of samples are tested in the present study: fine AP–binder matrixes, sandwiches (two-dimensional laminate propellants with alternating layers of AP and matrix laminas), and propellants. The matrixes contain AP in one of four different size ranges that are identified as 2, 10, 75, and 200 μm. The 2-μm AP was supplied by Thiokol Corporation, in the form of a mixture with uncured HTPB and dioctyl adipate–plasticizer (DOA); it was in the size range of 1.6–2 μm approximately. The 10-μm AP was supplied by the U.S. Naval Air Warfare Center (Weapons Division); it was in the size range of 10–15 μm approximately. The 75-μm and the 200-μm AP are obtained by passing as-received Kerr McGee AP through pairs of standard sieves with mesh openings of 75 and 90 μm for the former and 180 and 225 μm for the latter. The AP content in the matrixes is at the 65% level. The binder composition is HTPB = 75.73%, DOA = 18.39%, IPDI = 5.88%. The beakers containing the mixed matrix samples were slowly rotated ($\sim$1 rpm) during curing to prevent the AP particles from settling down due to gravity.

The sandwiches use pressed pellets of AP as outer lamina, in between which is a lamina of the matrix with the composition already mentioned. The pellets are prepared by compacting AP particles at a pressure of 220 MPa for 2 h. These particles are obtained by grinding as-received Kerr McGee AP for 8 min in a vibrating mill and have an average size of around 60 μm with a wide-cut distribution. The 2- and the 10-μm AP are used in the matrix lamina of the sandwiches. Three levels of matrix lamina thickness are tested in the present study: thin ($\sim$100–150 μm), intermediate ($\sim$250–275 μm), and thick ($\sim$450–600 μm).

Two propellant formulations are tested in the present study. Both have a solids loading at 87.5% and use the matrix composition mentioned earlier. The 2- and the 10-μm AP are used in the matrixes of the two propellant formulations. The coarse AP, constituting the remainder of the solids, is in the 355–425 μm size range in both formulations. The propellants are processed using a micromixer and degasser developed in-house and described elsewhere,[10] according to procedures detailed in Ref. 10. The error in the weighing of the ingredients during mixing of the all of the matrixes and propellants used in the present study is within 0.5%.

The matrix samples are about 7 mm tall and have cross-sectional dimensions of 6×4 mm approximately. The propellant samples are of similar cross-sectional dimensions, but are about 12 mm tall. The greater height is required to obtain sufficient number of video frames for the determination of the propellant burning rate because they burn faster than the matrixes. The propellant samples are coated with a thin layer ($\sim$1 μm approximately) of high-vacuum grease to inhibit the sides from burning. This is not done with the matrix samples, because it might affect their flammability, which itself is the subject of investigation in the present study. The sandwich samples are around 10 mm tall, 3 mm thick, and 2 mm wide. The width is governed by the thickness of the pressed AP pellets, which is considered sufficient based on several previous studies (e.g., Ref. 9), where it is observed that the processes that govern the sandwich burning rate are confined to a region around 100–150 μm into the AP lamina from its interface with the matrix lamina. The edge effects on AP deflagration at the outer edges of the sandwich do not influence the governing processes around the matrix lamina either.

Methods

Two techniques are primarily used in the present study: 1) combustion photography and 2) scanning electron microscopy (SEM) of quenched samples. These techniques are routine and are detailed elsewhere.[11] The combustion photography experiments are performed in a window bomb, and the combustion event is imaged using either a standard color video camera operating at 30 frames per second, or a high-speed digital camera (Redlake Imaging) up to a maximum of 1000 frames per second. Burning rates are obtained from the combustion photography experiments based on a frame-by-frame analysis of the color video images. The displacement between the points of maximum regression on the burning surface along the direction of flame propagation is noted in successive frames. This takes into account the nonplanar nature of the surface regression of the samples tested in the present study. A correlation coefficient $>$99.9% is stipulated for fitting a straight line to the surface displacement data obtained as already described, plotted against the framing time. The slope of the straight line, adjusted for the magnification of the images, yields the burning rate. Approximately 50% of the data are tested for repeatability within 5%, as a rule. Besides, data for the propellant samples are obtained at shorter pressure intervals [limited by the least count of the pressure gauge used, which is 0.345 MPa (50 psig)], to confirm the observed burning rate trends.

In the high-speed imaging experiments, the matrix and propellant samples are cut at $\sim$45 deg to the direction of flame propagation, and ignition is effected at the bottom edge of the cut surface. The line of view of the camera is, thus, oblique to the burning surface. This is to obtain a direct view of the burning surface. However, a tradeoff is necessitated between high magnification and the shallow depth of focus across the slant burning surface that it entails. A blue Kodak Wratten filter is fitted to the camera when testing sandwiches and propellants to filter out all radiation (especially from soot) except that corresponding to CH chemiluminescence, which is representative of the gas-phase reaction zone.

Quenched samples are obtained by rapid depressurization under conditions when the samples burn to completion. The rapid depressurization quench technique is the same as that developed at the U.S. Naval Air Warfare Center (Weapons Division) and at this laboratory. The depressurization rate employed has been estimated as $\sim$690 MPa/s ($\sim 10^5$ psig/s) (Ref. 12). Rapid depressurization has been observed to cause the formation of an extremely thin layer ($<$1 μm) of binder covering very fine AP particles in the matrixes. This could be due to mild foaming of the binder immediately after the depressurization quench. Dramatic effects of depressurization such as shattering of molten binder layers has consistently not been observed in the hundreds of samples examined by these authors over several years. Self-quenched samples, mostly those of matrixes in the extinction regime, are also examined in the SEM.

Results and Discussion

Matrixes

Burn/No-Burn Domains

The flammability regions of matrixes are shown in Fig. 1. Three types of burning behavior are observed with these samples, which are indicated in Fig. 1 as burn, quench, and no burn. The first signifies that the sample burns to completion. Quench indicates that the sample burns for some time after ignition, before self-quenching. This usually occurs within half the length of the sample, in the

present study. The length of the sample used is considered appropriate based on this observation. The no-burn condition implies that the sample does not continue to burn, or barely burns, after the ignition event. Figure 1 shows that the matrixes exhibit an interesting pattern of burn/no-burn behavior, wherein the pressure level corresponding to a midpressure extinction of the matrix increases with the size of the AP particles in it. Two matrixes, with 2- and 10-μm AP, have been chosen for further examination in the present work based on this behavior. The 2-μm AP matrix burns in a narrow pressure range of 2.07–2.42 MPa (300–350 psig), whereas the 10-μm AP matrix burns over a larger pressure range, namely, 1.38–3.45 MPa (200–500 psig).

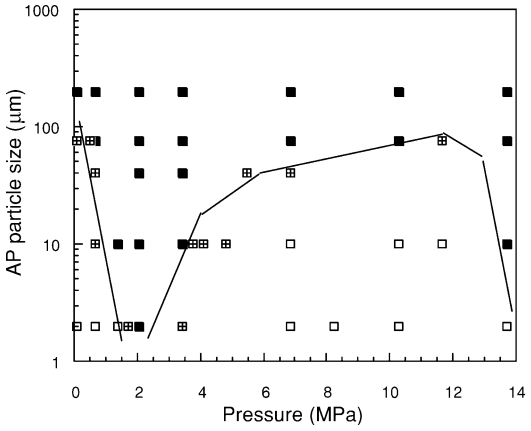

Fig. 1 Burn/no-burn domains of the fine AP/binder matrixes: ■, burn; ⊞, quench; and □, no burn.

Note that the matrix flammability behavior is a function of the cross-sectional area of the sample. Screening tests have been performed by the present authors with different sample sizes. It is found that samples that are substantially bigger (by twice) than those routinely used in the present study do not show differences in the flammability limits than what is reported in Fig. 1. On the other hand, smaller samples have indeed indicated larger no-burn regions than observed in Fig. 1. This was recognized early on by Bastress.[2]

High-Speed Images

The burning of the matrixes with the 2- and the 10-μm AP particles in narrow pressure ranges around their respective burn/no-burn boundaries shown in Fig. 1 are imaged with a high-speed camera. Selected frame sequences are shown in Fig. 2. The burning is, on the whole, extremely sporadic and transitory, and the burning surface regresses in an extremely non-uniform manner in the pressure range just around the burn/no-burn boundary in each case. In general, no specific event is witnessed in the high-speed images that could be considered as triggering the extinction in the self-quenching samples. A sharp boundary cannot, therefore, be attributed to this phenomenon. However, it can be observed in Fig. 2 that the burning surface is relatively planar at the lower pressure when compared to that at the higher pressure [the pressure difference being 0.35–0.69 MPa (50–100 psig)]. The extent of nonuniformity is much larger than the size of the particles contained in the matrix.

There is no visible flame over most parts of the burning surface most of the time during its regression, except for the occasional

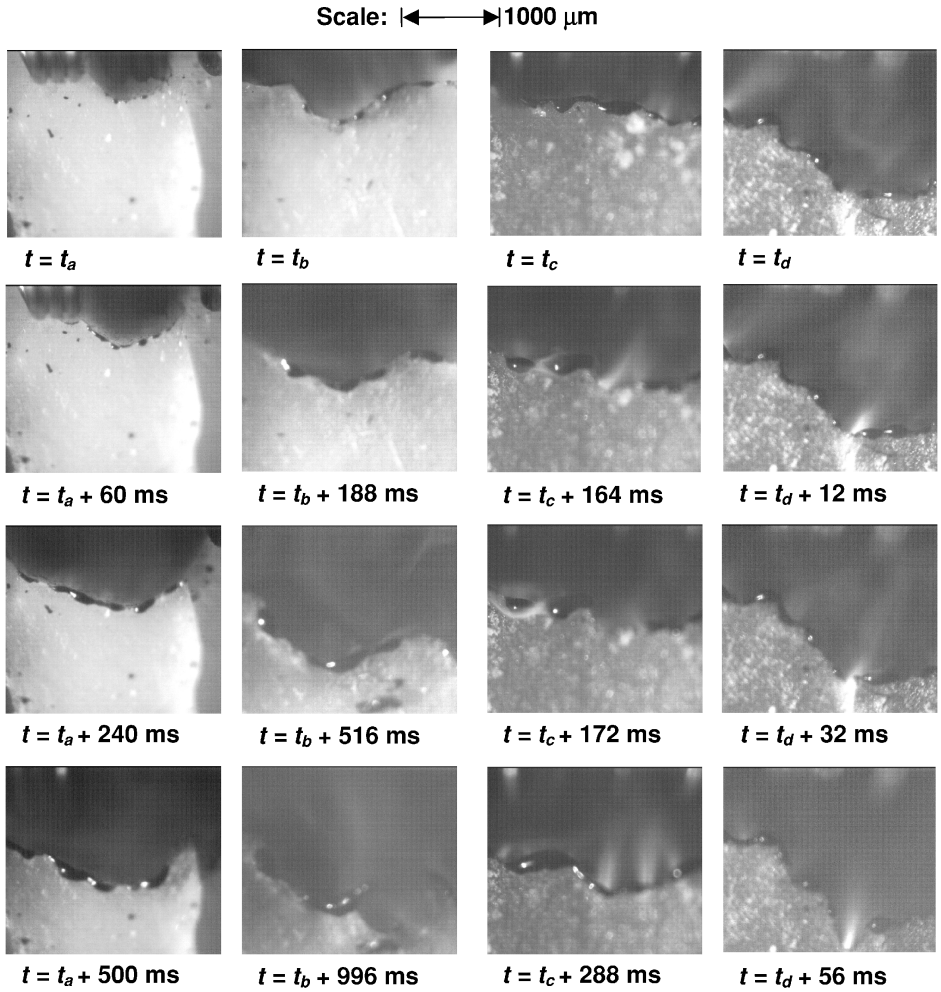

a) 2-μm AP matrix at 2.76 MPa (400 psig) **b) 2-μm AP matrix at 3.45 MPa (500 psig)** **c) 10-μm AP matrix at 3.45 MPa (500 psig)** **d) 10-μm AP matrix at 3.79 MPa (550 psig)**

Fig. 2 Frames from high-speed combustion photography of matrixes across the burn/no-burn boundary.

presence of microflamelets that could be identified with burning of dark beads of what appear to be binder melt drops along the edges of the burning surface. The melt drops accumulate and grow along the sample edges as the burning progresses. This is an artifact of the finite size of the sample. However, it indicates the presence of the binder in molten form on the burning surface. The molten binder may flow around locally, which causes its accumulation in parts close to the sample edge. Because the melt drops are formed along all of the edges of the sample, it may be deduced that the flow is driven by surface tension such as in capillary action and not by gravity, considering that the burning surface is initially inclined toward the camera. The binder motion could also be induced by the gas jets due to the decomposition of the fine AP particles from beneath the melt layers, but this is not apparent with the spatial resolution afforded by these images. Comparing the images of the 2- and the 10-μm AP matrixes, greater prevalence of microflamelets can be observed with the latter matrix.

There are two effects that need to be considered in this context: the effect of the binder melt flow on the AP particles and vice versa. Whereas the finer particles are affected more by the binder melt flow as their size is relatively comparable to the melt layer thickness, they also tend to impede the flow of binder over larger distances, by acting in a way similar to a gellant. The greater prevalence of the melt drop-related microflamelets with the larger particles in the matrix indicates that these particles do not impede the melt flow as much.

Quenched Surfaces

Quenched surfaces of the matrixes with 2- and 10-μm AP are examined as a function of pressure in a range closely around their respective burn/no-burn boundaries indicated in Fig. 1. Figure 3 shows the quenched surfaces of samples that burn to completion (depressurization quenched) and those that undergo self-quenching. The chief difference between the two is the prominent presence of large pits, regions of accelerated regression at quench, in the self-quenched samples. These regions are of length scales much larger than the AP particle size in the samples. Actually, the depressurization-quenched samples also indicate such regions, although to a much smaller extent; they are not so deep and wide. This indicates that a tendency for locally nonplanar burning exists sporadically even at pressures approaching the burn/no-burn boundary, but such tendency is accentuated in the no-burn domain and is perhaps the cause of the self-quenching process itself. Large regions of binder melt layers over regions with AP particles are present in the depressurization-quenched samples. Note that the length scales of the melt flow patterns are larger for the 10-μm AP matrix than for the 2-μm AP matrix. This is consistent with the observation of the greater prevalence of the melt drop-related microflamelets in the high-speed images. On the other hand, the self-quenched samples indicate considerable redistribution of the AP particles, accumulation in some areas and depletion in others, more with the 2-μm AP than the 10-μm AP. Correspondingly, the regions of accelerated regression are larger in extent for the 2-μm case than for the 10-μm case. The regions of accelerated regression in the depressurization-quenched samples also exhibit redistribution of AP particles to some extent.

Processes Governing Matrix Extinction

In the attempt to explain qualitatively the matrix burning characteristics described, the question arises as to what causes considerable amount of binder to accumulate on the burning surface relative to the AP particles, regardless of its molten nature. It is known that the activation energy of surface pyrolysis of AP is greater than that of the binder.[7] This implies that the pyrolysis rate of AP is more sensitive to its surface temperature than that of the binder. The surface temperature increases with increase in pressure due to faster chemical reaction rates and heat release rates in the gas phase at higher pressures. The surface temperature increases by about 100 K over a pressure range of interest here, that is, ~2.07–8.27 MPa (300–1200 psi) (Ref. 13), but this is considered significant for the purpose of the present discussion. Thus, the AP particles tend to

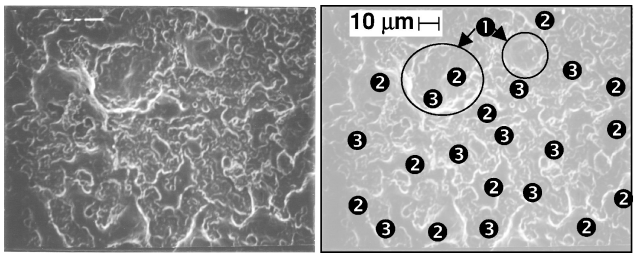

a) 2-μm AP matrix depressurization quenched at 2.07 MPa (300 psig): 1) regions of relatively accelerated regression, 2) binder melt layers, and 3) regions with AP particles

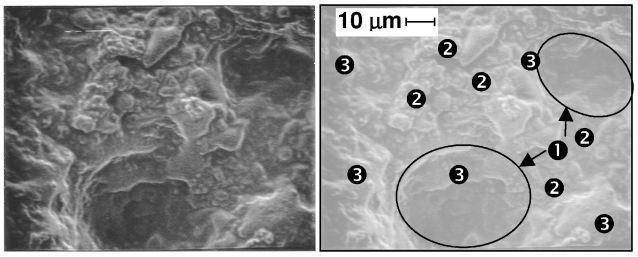

b) 2-μm AP matrix self-quenched at 2.76 MPa (400 psig): 1) large regions of accelerated regression, 2) regions of particle accumulation, and 3) binder surface layers bereft of AP particles

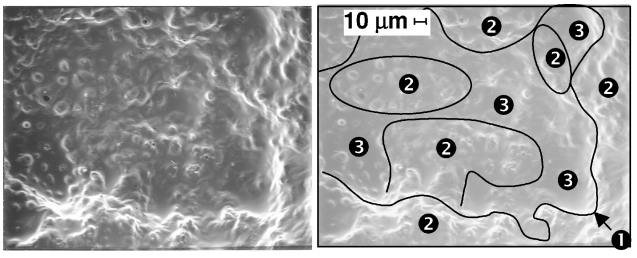

c) 10-μm AP matrix depressurization quenched at 3.45 MPa (500 psig): 1) region of retarded regression, 2) accumulation of AP particles in protruded regions, and 3) regions of binder with low concentration of particles

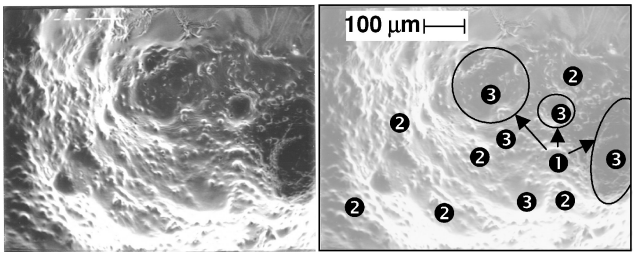

d) 10-μm AP matrix self-quenched at 4.13 MPa (600 psig): 1) large regions of accelerated regression, 2) regions of accumulated AP particles, and 3) regions of binder with low concentration of particles

Fig. 3 Surface features of matrixes across the burn/no-burn boundary.

pyrolyze faster relative to the binder as the pressure is increased. This is generally observed in the form of protrusion of AP particles on the burning surface at low pressures and their recessed appearance at high pressures in the noted pressure range. Correspondingly, the binder accumulates on the burning surface relative to the AP particles, as the pressure is increased. The process of relative accumulation of the ingredients is necessary for a steady propagation of the combustion wave because the slower pyrolyzing ingredient protrudes/accumulates and exists closer to the heat source, that is, the gas-phase flame, to increase its temperature and match the pyrolysis rate of the faster pyrolyzing ingredient. This was recognized earlier by Bastress[2] and Deur and Price.[14]

It is then postulated here that the unsteadiness associated with the extinction of the matrix burning is due to the response of the gas-phase flame to perturbations in the relative accumulation of the ingredients on the burning surface. It is reasonable to suppose that

matrixes with fine AP particles burn in a premixed flame in the pressure range of interest.[15] Note that the flame is generally of fuel-rich stoichiometry. A shift toward a stoichiometric mixture fraction would cause the flame to exist closer to the burning surface due to increased heat release rates and vice versa. Let us consider a perturbation of the relative accumulation of the ingredients on the burning surface toward a more fuel-rich situation. The gas-phase flame then tends to move farther away from the burning surface, causing the surface temperature to decrease. This results in a greater decrease in the pyrolysis rate of the AP than that of the binder because of its greater pyrolysis activation energy. This causes an increase in the accumulation of the AP particles when compared to the perturbed state, thus, restoring the original state of relative accumulation of the ingredients. It can be argued in a similar manner that the pyrolysis of AP–binder mixtures with oxidizer-rich stoichiometry is intrinsically unstable over the entire pressure range of interest. This would mean a progressively accelerated or retarded regression of the burning surface, as can be seen in the self-quenched samples in Fig. 3. This is not macroscopically verifiable because, in practice, AP–HC propellants and matrixes that are used in rocket applications are inherently of overall fuel-rich stoichiometry. As such, it appears that the AP particles are redistributed by binder melt flow in a microscopic manner to achieve locally oxidizer-rich proportions in the gas phase. This is observed to a limited extent even in samples that burn to completion, as in the case of the depressurization-quenched surfaces shown in Fig. 3. The microflow of the binder melt is supported by the high-speed images in Fig. 2. The regions of retarded regression drain heat laterally from the regions of accelerated regression, causing local quenching of the latter regions, eventually leading to self-quenching of the sample.

The foregoing arguments are based on static stability considerations. The dynamic stability aspect has to be worked out by solving the conservation equations of species and energy in a time-resolved manner. This is presently being addressed by one of the authors. The results indicate regimes of intrinsically oscillatory pyrolysis besides monotonically stable or unstable regimes implied in the given description.

A simpler argument than what is outlined for the extinction of the matrix may be that the binder melts and flows over the fine AP particles and covers the latter. Such an argument would imply that the self-quenched samples would have an overall smooth appearance due to the preponderant melt coverage of the surface ultimately. The presence of deep, large pits and accumulation of AP particles on parts of the surface cannot be completely explained by this view.

Sandwiches

Burning Rates

The variation of burning rate with pressure for sandwiches containing the 2- and the 10-μm AP matrixes is shown in Fig. 4. These sandwiches have an intermediate matrix lamina thickness of

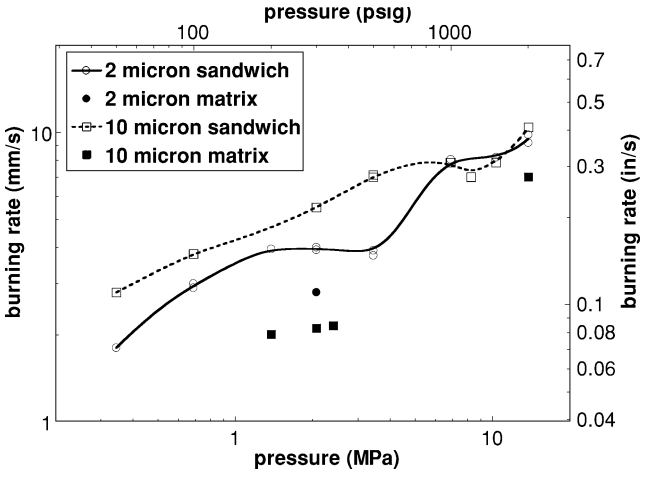

Fig. 4 Burning rates of sandwiches and their corresponding matrixes tested alone, matrix lamina thickness in sandwiches ~250–275 μm.

~250–275 μm (corresponding to maximum burning rate when the matrix lamina thickness is varied at constant pressure). The burning rates of the matrixes burning alone are also shown in Fig. 4 for comparison. It can be seen that the sandwich with the 2-μm AP matrix exhibits a plateau in the pressure range slightly above the onset of extinction of its matrix when tested alone. Similarly, the sandwich with the 10-μm AP matrix exhibits a plateau in the pressure range slightly above that corresponding to the extinction of its matrix. The slightly higher pressure is most probably due to the assisted heating by the O/F flame associated with the AP lamina–matrix interface. A relatively low pressure exponent of the burning rate of the 2-μm-matrix sandwich at elevated pressures [6.9–13.8 MPa (1000–2000 psig)] is not considered to be directly related to the matrix extinction and is perhaps due to other mechanisms, notably the one detailed in Ref. 9, as mentioned earlier.

High-Speed Images

The high-speed imaging of sandwich burning is performed for the three designated matrix lamina thickness levels over pressure ranges corresponding to anomalous burning rate trends of the sandwiches observed in Fig. 4. The framing rate in these tests is 125 frames per second.

Expectedly, the sandwiches with the thin- and the intermediate-thickness laminas of either the 2- or the 10-μm AP matrix do not show substantial differences in the burning behavior as the pressure is increased across their respective test pressure ranges. The spatial resolution is not adequate to resolve any such differences. By contrast, the thick-matrix sandwiches do indicate some interesting features of burning behavior as the pressure is increased. Figure 5a shows one frame each of the 2- and 10-μm AP matrix sandwiches with thick-matrix laminas burning at the low end of their respective test pressure ranges. These frames are representative of all of the frames obtained during the burning of the respective samples. On the other hand, sets of consecutive frames of these samples burning at the high end of their test pressure ranges are shown in Fig. 5b, to highlight the transitory behavior of the flame structure. The lamina contact edges are artificially highlighted with white lines for clarity in all of these images.

The overall profile of the sandwich burning surface is symmetric in Fig. 5a, but significantly asymmetric in the images shown in Fig. 5b. Asymmetric burning of pure binder sandwiches has been reported extensively with binders that are particularly prone to substantial melting before decomposition.[16] Close observation of the images in Fig. 5b shows the existence of dark beads of melt drops along the front edge of the matrix burning surface, indicating the presence of molten binder. This feature is not as extensive as with the matrixes tested alone, due to the relatively small amount of the matrix present in the middle lamina of the sandwich samples.

The burning-surface profile of the matrix lamina exhibits little or no protrusion in Fig. 5a, whereas substantial protrusion of the matrix lamina is observed in Fig. 5b. It can also be seen that the two leading edges of the O/F flame anchored to the lamina contact planes are connected together within a short distance from the matrix burning surface in Fig. 5a. The intensity of the flame subsequently downstream is uniformly bright (not saturated) within the field of view shown here. On the contrary, in Fig. 5b, the two leading edges of the O/F flame remain disconnected for large distances from the matrix burning surface in general. This is particularly pronounced with the 10-μm AP matrix sandwich, as seen in the first frame of this sample burning in Fig. 5b. The consecutive frames for both the matrix sandwiches in Fig. 5b show momentary establishment of a connection between the two leading edges of the O/F flame closer to the burning surface of the matrix lamina. This is due to the intermittent nature of the burning of the matrix laminas in the sandwiches at the high ends of their respective test pressure ranges.

Quenched Surfaces

The sandwiches are quenched by rapid depressurization at similar test pressures as already described. Figure 6 shows an array of quenched surfaces to illustrate the effect of the matrix lamina thickness, the fine AP particle size, and the pressure.

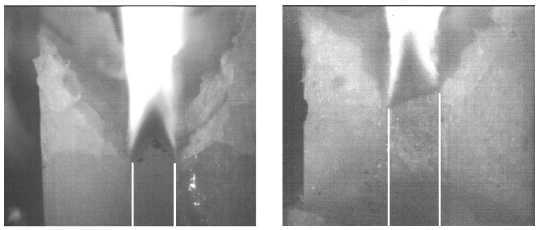

a) Low end of test pressure range

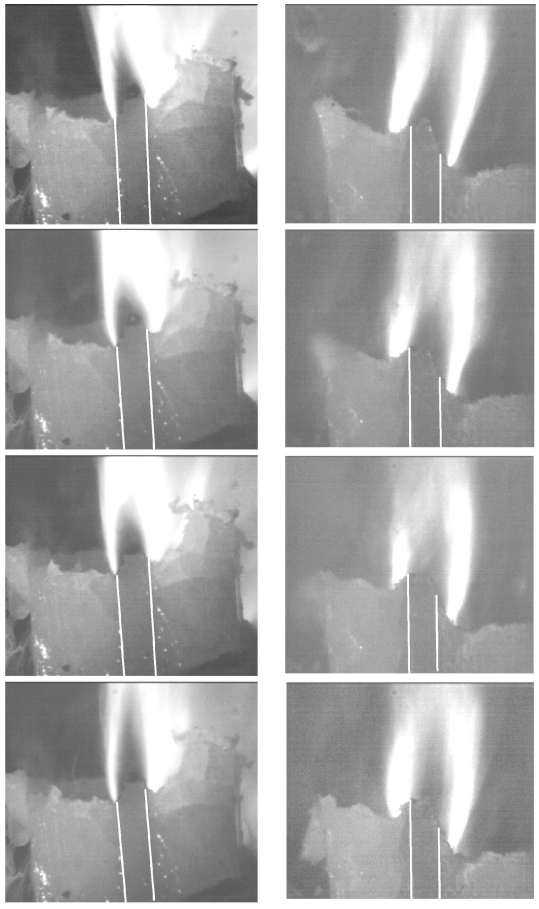

b) High end of test pressure range

Fig. 5 Frames of high-speed combustion images of burning of sandwiches with thick matrix laminas; lamina interface edges artificially marked with white lines for clarity.

The thin-matrix lamina sandwiches (not shown here) do not exhibit major differences with variation of pressure as in the case of the high-speed images. The matrix lamina surface is flat and recessed relative to the adjacent AP laminas at the lower end of the test pressure range for both matrix sandwiches, compared to that at the higher end. Ripples of binder melt are evident, and large pits (with size of the order of the matrix lamina thickness) are observed sporadically at the higher end of the test pressure range. Redistribution of the fine AP particles on the matrix surface is observed under all conditions, particularly more at the higher end of the test pressure range for each matrix sandwich.

In the case of sandwiches with the intermediate lamina thickness, the differences between the low end of the test pressure range and the high end are apparent, as seen in Figs. 6a and 6b. The surface of the matrix lamina is recessed on the whole relative to the adjacent AP laminas at the low end of the test pressure range [4.13 MPa (600 psig)] in Fig. 6a, with small-scale variations of protrusion and recession as observed in the context of the matrix tested alone (Fig. 3c). On the other hand, the surface of the matrix lamina at 5.51 MPa (800 psig) in Fig. 6b has a somewhat smooth appearance, with a greater extent of unevenness, and ripples of binder melt flow. The AP particles are found as lumps buried under the binder, in this case.

The differences between the surface features at the low and high ends of the test pressure ranges for the two matrix sandwiches are the most significant for the thick-matrix–lamina sandwiches. Under all conditions, the thick-matrix–lamina sandwiches show significant protrusion of the matrix lamina somewhere in the middle of the matrix, but not exactly symmetric about the two lamina contact planes. However, the surface along the slopes of the protruding matrix is relatively even microscopically at the low-pressure end (not shown here), with a somewhat dry appearance exhibiting accumulation of AP particles, similar to what is seen in Fig. 6a. On the contrary, the matrix surface at the high-pressure end exhibits large-scale regions of accelerated and retarded regression within the width of the lamina, as can be seen in Figs. 6c and 6d for the two matrix cases tested in the present study. Significant clumping of the 2-μm AP particles and redistribution of the 10-μm AP particles along the slopes of the protruded regions can be observed in Fig. 6c, indicating nonuniform burning of the matrix laminas at the high ends of their respective test pressure ranges.

Effect of Matrix Burning Behavior on the Burning Rate of Sandwiches

Regardless of whether the matrix burns or not anywhere in the pressure range, the O/F flame associated with the contact lines between the matrix and the AP laminas in the sandwiches sustain the combustion, in the pressure range of interest. In fact, the leading edge of the O/F diffusion flame in the mixing fan associated with the lamina contact planes [designated as the lamina leading-edge flame (LLEF) in previous studies[17]] controls the burning rate of the sandwich even when the matrix lamina burns on its own, as could be seen from the sandwich burning rates being higher than the matrix burning rate when tested alone, even with very large matrix lamina. However, the presence or absence of the matrix flame has been found to be crucial in influencing the multidimensional interaction between the two LLEFs anchored to the adjacent lamina contact planes in the sandwiches.

In the past studies,[17] tests were done with sandwiches containing matrixes of the 10-μm AP with poly-butadiene acrylonitrile acrylic acid binder in the ratios of $\frac{7}{3}$ and $\frac{5}{5}$. The $\frac{7}{3}$ matrix undergoes self-sustained burning in the pressure range of interest to the present study, but the $\frac{5}{5}$ matrix does not. The $\frac{7}{3}$ matrix sandwiches show significantly pronounced peaks in the burning rate as the matrix lamina thickness is varied at constant pressure, when compared to the $\frac{5}{5}$ matrix sandwiches. This observation has not been explained adequately earlier. The peak in the burning rate variation vs matrix lamina indicates an enhanced coupling between the LLEFs in terms of two-dimensional heat feedback to and consumption of reactants from across the matrix lamina. When the matrix is capable of self-sustaining combustion when tested alone, its premixed flame would connect the fuel-rich sides of the adjacent LLEFs in the sandwich configuration (referred to as the canopy flame[17]). The presence of the premixed flame is conducive to preheating the reactants in the central parts of the matrix lamina, which would increase the thermal conductivity of the gases in the flame standoff region all across the matrix lamina and enhance the two-dimensional heat feedback from the LLEFs. This results in a pronounced peak in the burning rate variation vs matrix lamina thickness, relative to when the matrix does not support a flame by itself.

When the pressure is increased across the burn/no-burn boundary of the matrix (or at slightly higher pressures as noted earlier), the processes such as intermittent burning described in the context of matrix extinction would indeed occur. However, the matrix does not really extinguish, because its ingredients pyrolyze with the heat from the LLEFs, and the pyrolysis products from the central parts of the matrix lamina contribute to the outer diffusion flame trailing off from the LLEFs. The intermittent burning behavior of the matrix lamina

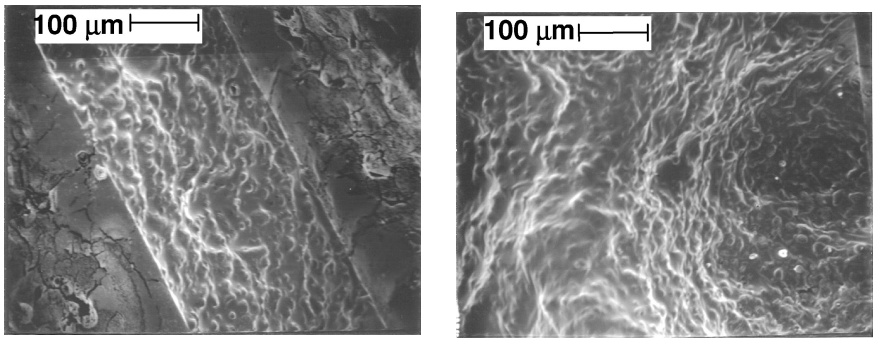

a) Intermediate lamina thickness of 10-μm AP matrix quenched at 4.13 MPa (600 psig)

c) Thick lamina of 10-μm AP matrix quenched at 5.51 MPa (800 psig)

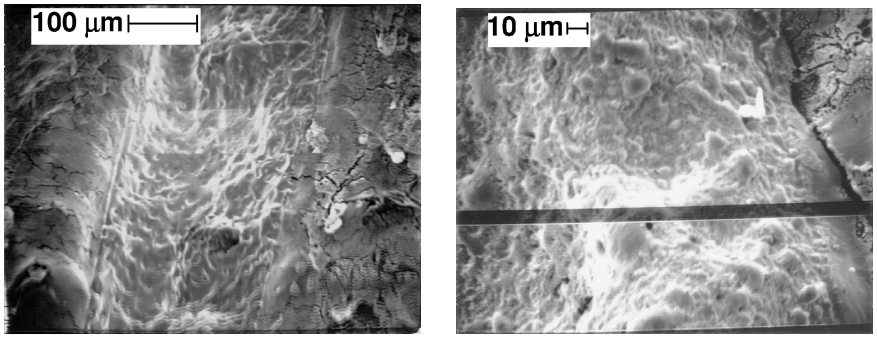

b) Intermediate lamina thickness of 10-μm AP matrix quenched at 5.51 MPa (800 psig)

d) Thick lamina of 2-μm AP matrix quenched at 3.45 MPa (500 psig)

Fig. 6 Surface features of sandwiches.

of the sandwich is indeed observed in Fig. 5b. Such a transitory flame over the matrix lamina is not conducive to increasing the two-dimensional heat feedback from the LLEFs to the burning surface, resulting in a low burning rate or lack of increase in the burning rate commensurate with increase in the pressure. This results in a low-pressure exponent of the burning rate in the pressure range corresponding to the onset of extinction of the matrix tested alone, as seen in Fig. 4.

Role of the Matrix Lamina Thickness

With the canopy premixed flame over the matrix lamina becoming intermittent, the decreased coupling between the adjacent LLEFs is most prominent in sandwiches with the intermediate range of matrix lamina thickness than those with thin- or thick-matrix laminas.[17] The intermittent burning behavior of the matrix lamina in the intermediate thickness range is not conclusively observable, but such behavior is quite apparent with thick laminas of the matrix. The nonplanar burning surface associated with the intermittent burning of the matrix is observed with intermediate thickness of the matrix lamina in the sandwich quenched surfaces (Fig. 6), however.

Propellants

Burning Rates

Figure 7 shows burning rates of the family of two propellant formulations tested in the present study. Both propellant formulations clearly exhibit plateau burning in a relatively high-pressure range, 6.89–13.78 MPa (1000–2000 psig). However, this aspect is not the focus of the present study but has been studied in companion work of the authors.[9] Rather, we concentrate on the occurrence of plateaus in an intermediate pressure range.

The 2-μm fine AP formulation barely exhibits a plateau (one datum point) in the midpressure range, 2.76–3.10 MPa (400–450 psi), corresponding to the onset of the matrix extinction in Fig. 1. Although the processes relating the interaction of the intermittent burning of the matrix with the LEFs attached to the adjacent coarse particles could still be prevalent as in the sandwiches, its contribution in determining the burning rate trend with pressure would be mitigated by the inherent intermittency of propellant burning due

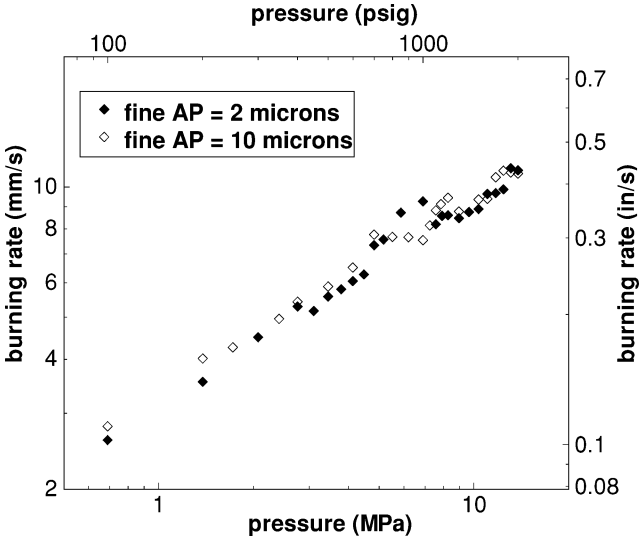

Fig. 7 Burning rates of bimodal propellants.

to burn out of coarse particles and burning of new ones emerging from beneath the burning surface. For the 10-μm fine AP propellant formulation, however, a plateau in the burning rate is observed over 4.82–6.89 MPa (700–1000 psig). [Note that the high-pressure plateau occurs at a slightly higher pressure in this case than with the 2-μm fine AP formulation and is separated from the midpressure plateau by about 2.07 MPa (300 psig).] The occurrence of the midpressure plateau is in the pressure range slightly higher than the onset pressure of the corresponding matrix extinction, similar to that observed in the sandwiches, and also as reported by Foster and Miller.[1]

High-Speed Images

High-speed imaging of the combustion of the preceding bimodal propellants is performed at distinct test pressure levels in relation

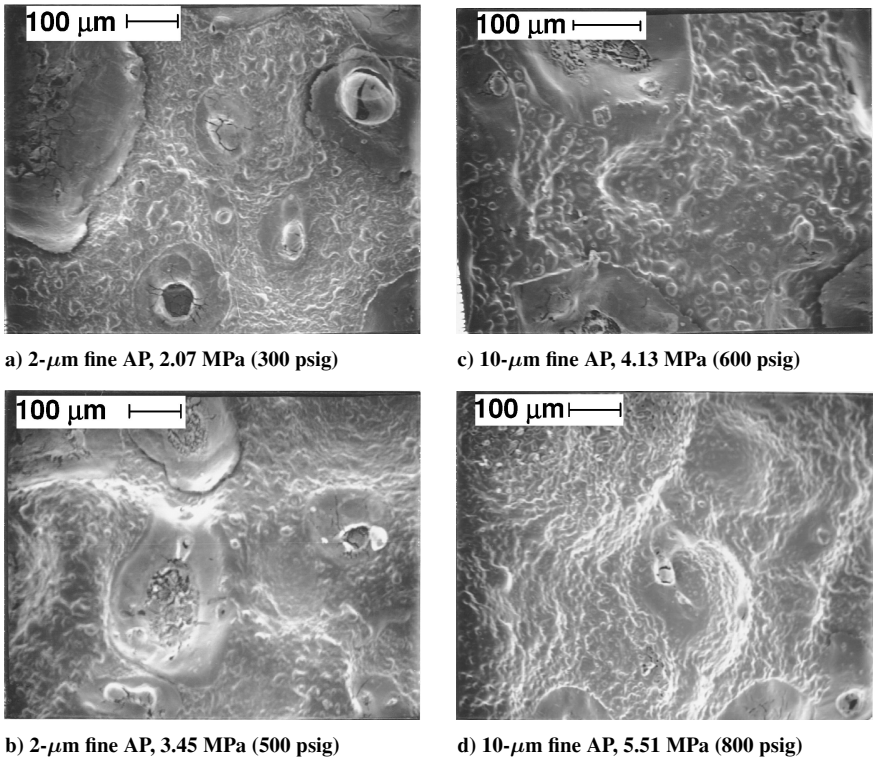

a) 2-μm fine AP, 2.07 MPa (300 psig) **c) 10-μm fine AP, 4.13 MPa (600 psig)**

b) 2-μm fine AP, 3.45 MPa (500 psig) **d) 10-μm fine AP, 5.51 MPa (800 psig)**

Fig. 8 Surface features of bimodal propellants.

to the onset of extinction of their respective matrixes, as in the case of the sandwiches. It is very difficult to discern intermittent burning of matrix areas on the burning surface in between coarse AP particles in these images, with the prevalence of an inherently unsteady burning process at the scale of the coarse AP particle size, as already mentioned. In view of this, the images are not shown here. However, it has been possible to locate momentarily dark areas or transitory dark patterns with length scales substantially greater than the coarse AP particle size (400 μm) in the propellants, which could indicate intermittent burning of the matrix in locations that just emerged on the burning surface after the burn out of a coarse particle. It is not possible to distinguish differences in the intermittent burning behavior as the pressure is increased over the test pressure ranges for the two propellant formulations tested here.

Quenched Surfaces

Figure 8 shows surface features of the two bimodal propellants quenched in the pressure ranges of the onset of extinction of their respective matrixes when tested alone. It can be seen that the matrix surface in the propellants is relatively planar at the low end of the plateau pressure range when compared to the high end. Significant accumulation of fine AP particles on the burning surface is observed at the low end of the pressure range when compared to the high-end case. Binder melt layers with length scale of the order of 10 μm are seen sporadically on the 2-μm-AP matrix surface at 2.07 MPa (300 psi) in Fig. 8a, similar to the observation in Fig. 3a for the matrix tested alone. At the high end of the pressure range, large local regions of accelerated or retarded regression are seen, similar to the surface features of the self-quenched matrix (Figs. 3b and 3d). Accumulation and depletion of fine AP particles coincide with these protruded and recessed regions on the matrix burning surfaces.

Role of the Coarse AP Particle Size

The size of the coarse AP particles dictates the spacing between them in the propellant microstructure and plays a role similar to the matrix lamina thickness in the sandwiches considered earlier. The use of 400-μm coarse AP particles in the present propellant formulations is significant, because the distance between the adjacent coarse particles predominantly falls in the intermediate matrix lamina thickness range for the given fine AP content.

Conclusions

Burning of composite solid propellants based on AP oxidizer of a widely separated bimodal particle size distribution involves substantial areas of the burning surface layer being made up of a matrix of fine AP particles and binder. Appropriate combinations of matrix variables result in a scenario of extinction of the matrix when tested alone in an intermediate-pressure range. Examination of quenched surfaces and high-speed combustion photography of such matrixes, and sandwiches and propellants containing those matrixes, reveals the onset of large-scale non-uniform burning as the pressure is increased across the matrix burn/no-burn boundary. The non-uniform burning is accompanied by binder melt flow and a local redistribution of the fine AP particles along nonplanar patterns on the burning surface. These processes cause the pyrolysis behavior of the matrixes to be unstable and form the basis for intermittent burning of the matrix when tested alone or in the sandwich and propellant samples. The intermittency in the matrix flame influences the interaction between the leading-edge flames on adjacent AP laminas on coarse particles in the sandwiches and propellants in a manner that leads to low-pressure exponent or plateau burning rates of the sandwiches and propellants in the pressure range corresponding to the onset of matrix extinction when tested alone. This is more conspicuous in sandwiches than propellants due to the non-contiguous nature of the interfacial contact between the coarse AP particles and the matrix in the microstructure of the latter samples.

Acknowledgments

This work was supported by the U.S. Office of Naval Research under Contract N00014-99-1-1055 with Judah Goldwasser as Technical Monitor.

References

[1]Foster, R. L., and Miller, R. R., "The Influence of the Fine AP/Binder Matrix on Composite Propellant Ballistic Properties," *Proceedings of the 17th JANNAF Combustion Meeting*, CPIA Publ. 329, Vol. 3, Chemical Propulsion Information Agency, Laurel, MD, Oct. 1980, pp. 91–104.

[2]Bastress, E. K., "Modification of the Burning Rates of Ammonium Perchlorate Solid Propellants by Particle Size," Ph.D. Dissertation, Dept. of Aeronautics Engineering, Princeton Univ., Princeton, NJ, Jan. 1961.

[3]Steinz, J. A., Stang, P. L., and Summerfield, M., "Effects of Oxidizer Particle Size on Composite Solid Propellant Burning: Normal Burning, Plateau Burning, and Intermediate Pressure Extinction," Aerospace and Mechanical Sciences Rept. 810, Guggenheim Labs. for Aerospace Propulsion Sciences, Princeton Univ., Princeton, NJ, Oct. 1967.

[4]Summerfield, M., Sutherland, G. S., Webb, M. J., Taback, H. J., and Hall, K. P., "Burning Mechanism of Ammonium Perchlorate Propellants," *Solid Propellant Rocket Research*, ARS Progress in Astronautics and Rocketry, Vol. 1, Academic Press, New York, 1960, pp. 141–182.

[5]Miller, R. R., "Pressure Sensitivity and Non-Linearity in HTPB Propellants I. Effects of Aluminum Content and Solids Loading," *Proceedings of the 17th JANNAF Combustion Meeting*, CPIA Publ. 329, Vol. 3, Chemical Propulsion Information Agency, Laurel, MD, Oct. 1980, pp. 69–89.

[6]Miller, R. R., "Anomalous Ballistic Behavior of Reduced Smoke Propellants with Wide AP Distributions," *Proceedings of the 15th JANNAF Combustion Meeting* CPIA Publ. 281, Vol. 2, Chemical Propulsion Information Agency, Laurel, MD, Feb. 1979, pp. 265–269.

[7]Beckstead, M. W., Derr, R. L., and Price, C. F., "A Model of Composite Solid-Propellant Combustion Based on Multiple Flames," *AIAA Journal*, Vol. 8, No. 12, 1970, pp. 2200–2207.

[8]Cohen, N. S., and Hightower, J. O., "An Explanation for Anomalous Combustion Behavior in Composite Propellants," *Proceedings of the 29th JANNAF Combustion Meeting*, Chemical Propulsion Information Agency, Laurel, MD, Oct. 1992.

[9]Chakravarthy, S. R., Price, E. W., Sigman, R. K., and Seitzman, J. M., "Combustion of Ammonium Perchlorate–Polymer Sandwiches and Propellants at Elevated Pressures," *Journal of Propulsion and Power*, Vol. 19, No. 1, 2003, pp. 56–65.

[10]Sigman, R. K., Jeenu, R., and Price, E. W., "A Small-Scale Solid Propellant Mixer and Vacuum Degasser," *Proceedings of the 36th JANNAF Combustion Meeting*, Chemical Propulsion Information Agency, Laurel, MD, Oct. 1999.

[11]Chakravarthy, S. R., "The Role of Surface Layer Processes in Solid Propellant Combustion," Ph.D. Dissertation, School of Aerospace Engineering, Georgia Inst. of Technology, Atlanta, Georgia, Dec. 1995.

[12]Boggs, T. L., Price, E. W., and Zurn, D. E., "The Deflagration of Pure and Isomorphously Doped Ammonium Perchlorate," *Proceedings of the Thirteenth (International) on Symposium Combustion*, Combustion Inst., Pittsburgh, PA, 1971, pp. 995–1008.

[13]Zanotti, C., and Volpi, A., "Measuring Thermodynamic Properties of Burning Propellants," *Non-Steady Burning and Combustion Stability of Solid Propellants*, edited by L. De Luca, E. W. Price, and M. Summerfield, Progress in Astronautics and Aeronautics, Vol. 143, AIAA, Washington, DC, 1992, pp. 145–196.

[14]Deur, J. M., and Price, E. W., "Steady State One-Dimensional Pyrolysis of Oxidizer-Binder Laminates," AIAA Paper 86-1446, July 1986.

[15]Price, E. W., Chakravarthy, S. R., Sambamurthi, J. K., and Sigman, R. K., "Details of Combustion of Ammonium Perchlorate Propellants: Leading Edge Flame Detachment," *Combustion Science and Technology*, Vol. 138, 1998, pp. 61–81.

[16]Handley, J. C., "An Experimental Investigation of Catalysis in the Combustion of Composite Solid Propellants," Ph.D. Dissertation, School of Aerospace Engineering, Georgia Inst. of Technology, Atlanta, Georgia, March 1976.

[17]Lee, S.-T., Price, E. W., and Sigman, R. K., "Effect of Multi-Dimensional Flamelets in Composite Propellant Combustion," *Journal of Propulsion and Power*, Vol. 10, No. 6, 1994, pp. 761–768.